Energy & Environmental Science

Cite this: *Energy Environ. Sci.*, 2011, **4**, 1788

www.rsc.org/ees

PAPER

Enhanced light harvesting with π-conjugated cyclic aromatic hydrocarbons for porphyrin-sensitized solar cells

Chin-Li Wang,[a] Yu-Cheng Chang,[b] Chi-Ming Lan,[b] Chen-Fu Lo,[a] Eric Wei-Guang Diau*[b] and Ching-Yao Lin*[a]

Received 14th December 2010, Accepted 24th February 2011
DOI: 10.1039/c0ee00767f

Zinc porphyrins in a series bearing a phenylethynyl, naphthalenylethynyl, anthracenylethynyl, phenanthrenylethynyl or pyrenylethynyl substituent, denoted LD1, LD2, LD3a, LD3p or LD4, respectively, were prepared as photosensitizers for dye-sensitized solar cells. The overall efficiencies of the corresponding devices show a trend LD4 > LD3p > LD2 > LD3a > LD1. Significantly, LD4 features J_{SC}/mA cm^{-2} = 19.627, V_{OC}/V = 0.711, and FF = 0.721, giving an efficiency η = 10.06% of power conversion. This value is superior to that of a N719-based solar cell fabricated under similar experimental conditions. The remarkable performance of the LD4 cell is rationalized to be due to the broader and more red-shifted spectral feature that makes the IPCE spectrum to cover broadly across the entire visible region, 400–800 nm.

Introduction

Dye-sensitized solar cells (DSSCs) have attracted much attention because they present a highly promising alternative to conventional photovoltaic devices based on silicon.[1–5] In DSSC, efficiencies of conversion of light to electric power up to 11% have been obtained with polypyridyl ruthenium complexes.[6–8] Considerable effort is also being devoted to develop new and efficient sensitizers suitable for their modest cost, ease of synthesis and modification, large molar absorption coefficients and satisfactory stability. Among dyes under investigation, porphyrins are considered as efficient sensitizers for DSSC applications[9–28] because of the vital roles of porphyrin derivatives in photosynthesis, the strong absorption in the visible region, and the ease of adjusting the chemical structures for light harvest. Officer and co-workers reported a porphyrin-sensitized solar cell (PSSC) to attain an overall efficiency η = 7.1%.[13] Yeh, Diau and Gratzel *et al* reported a YD2-based PSSC with an overall efficiency of 11%.[15]

Our previous work on zinc porphyrins with phenylethynyl (PE) links of varied lengths (PE1–PE4) showed that the porphyrins with shorter links (PE1 and PE2) outperform those with longer links (PE3 and PE4).[21] Based on a structure similar to PE2, we incorporated further acenes in the bridge between the porphyrin core and the anchoring group (–COOH) to improve the light-harvesting ability, enabling the overall efficiency of the device with an anthracene-modified porphyrin to attain ~80% of the performance of a N719-based DSSC.[27] Our tests on various electron-donating or -withdrawing substituents added to PE1 revealed that a porphyrin sensitizer with *N*,*N*′-dimethylamino-PE

[a]*Department of Applied Chemistry, National Chi Nan University, Puli, Nantou Hsien, 54561, Taiwan. E-mail: cyl@ncnu.edu.tw; Fax: +886-49-2917956; Tel: +886-49-2910960 ext. 4152*
[b]*Department of Applied Chemistry and Institute of Molecular Science, National Chiao Tung University, Hsinchu, 30010, Taiwan. E-mail: diau@mail.nctu.edu.tw; Fax: +886-3-5723764; Tel: +886-3-5131524*

Broader context

Considered as a clean and unlimited renewable energy source, solar energy may play a key role to the future of mankind. Dye-sensitized solar cell (DSSC) has shown its potential as a feasible device for solar energy conversion. Recently, many studies have reported porphyrins as potential photo-sensitizers with comparable overall efficiencies to those of the Ru-based devices. In a systematic investigation to search for a highly efficient porphyrin dye, we found that the photovoltaic performance of a zinc porphyrin can be significantly improved by applying an anchoring group with a shorter linkage, by attaching a π-conjugated acene group to minimize the absorption gap, or by incorporating an electron-donating group into the π-conjugation system. As a continuous effort, we hereby report zinc porphyrin sensitizers modified by a series of cyclic aromatic hydrocarbon substituents. Among these dyes, a device made of pyrene-bearing zinc porphyrin (LD4) shows much improved photovoltaic performance, giving an overall efficiency 10.06% of power conversion. The superior performance of the LD4 dye is attributed to its enhanced light harvesting ability broadly covering the 400–800 nm region, which is a requirement for a panchromatic dye.

substitute improved an overall efficiency of PSSC further to attain ~90% of that of a N719 cell.[28] In the present work, we explore the possibility of improving the photovoltaic performance of PE1-sensitized solar cells by enhancing their light-harvesting ability through attaching various cyclic aromatic hydrocarbon substituents at the position opposite to the anchoring group of PE1. Anthracene, phenanthrene and pyrene molecules are effective candidates as substituents because of their strong emissions as probes in electron, energy or charge-transfer experiments[29–33] and because of their π-conjugated character to interact with the porphyrin core. As shown in Chart 1, the target porphyrins (denoted as LD1, LD2, LD3a, LD3p and LD4 for the cyclic aromatic substituents with phenylethyne, naphthalenylethyne, anthracenylethyne, phenanthrenylethyne and pyrenylethyne, respectively) are selected to test their spectral, photophysical and electrochemical properties so as to understand the device performance of the corresponding PSSC. We found that the cell performance exhibits a systematic trend showing LD4 > LD3p > LD2 > LD3a > LD1. The device made of LD4 showed a remarkable performance with J_{SC}/mA cm^{-2} = 19.627, V_{OC}/V = 0.711, and FF = 0.721, yielding an overall power conversion efficiency $\eta = 10.06\%$, which outperforms that of a N719-based DSSC fabricated with the same electrodes. This extraordinary J_{SC} performance of LD4 is due to its superior light-harvesting ability that extends the IPCE spectrum beyond 800 nm.

Experimental section

Materials

Air-sensitive solids were handled in a glove box (MBraun Unilab). A vacuum line and standard Schlenk techniques were employed to process air-sensitive solutions. Solvents for the synthesis (ACS Grade) were CH_2Cl_2 and $CHCl_3$ (Mallinckrodt Baker, KE USA), hexanes (Haltermann, Hamburg Germany) and THF (Merck, Darmstadt Germany). These solvents were used as received unless otherwise stated. Other chemicals were obtained from Acros Organics, NJ, USA. THF for cross-coupling reactions was purified and dried with a solvent purification system (Asiawong SD-500, Taipei, Taiwan); H_2O of about 50 ppm was found in the resulting THF. For electrochemical measurements, THF was distilled on sodium under N_2. $Pd(PPh_3)_4$ catalyst (Strem, MA, USA) and $Pd_2(dba)_3$ (Acros Organics, NJ, USA) were used as received. For chromatographic purification, we used Silica Gel 60 (230–400 mesh, Merck, Germany).

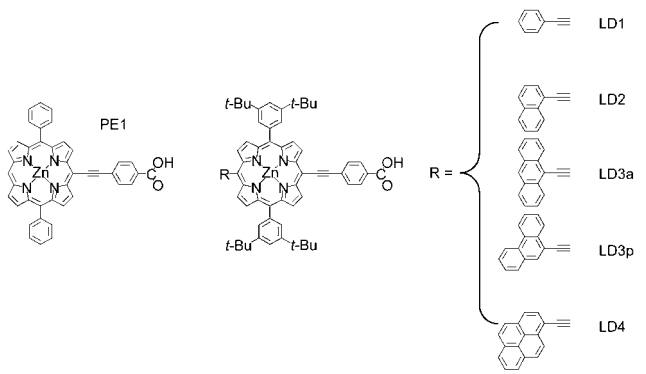

Chart 1 Molecular structures of PE1 and LD porphyrins.

Instruments

NMR spectra (Varian Unity Inova 300WB NMR Spectrometer), elemental analyses (Elementar Vario EL III, NSC Instrumentation Center at National Chung Hsing University), mass spectra (Microflex MALDI-TOF MS, Bruker Daltonics), electrochemical measurements (CHI Electrochemical Workstation 611A), absorption spectra (Agilent 8453 UV-Visible spectrophotometer) and fluorescence spectra (Varian Cary Eclipse fluorescence spectrometer) were recorded with the indicated instruments.

Compound synthesis and characterization

The target molecules were produced with the Sonogashira cross-coupling method:[34,35] typically, 5-bromo-10,20-bis(3,5-di-*tert*-butylphenyl)porphinato zinc(II) (100–150 mg) was mixed with suitable ethynyl substituents (0.83 equiv.), $Pd(PPh_3)_4$ (20 mol%), CuI (20 mol%) and Et_2NH (5 mL) in dried THF (70 mL) under dinitrogen. The degassed reaction mixtures were stirred under dinitrogen at 40 °C and monitored with TLC and UV-visible spectra. Upon completion, the reactions were quenched with $NH_4Cl_{(aq)}$ washes followed by chromatographic separation on silica gel with THF/hexanes as eluent and crystallization from THF/hexanes. Yields were 26, 36, 37, 30 and 30 percent for LD1, LD2, LD3a, LD3p and LD4 precursors, respectively. These precursors were reacted with 4-ethynyl-benzoic acid (3 equiv.) to afford the final products. After chromatographic separation on silica gel with MeOH/CH_2Cl_2 eluents and crystallization from THF/hexanes, 62, 68, 67, 59 and 69% of LD1, LD2, LD3a, LD3p and LD4 were collected, respectively.

LD1. ^{1}H NMR (DMSO-d_6 at 2.50 ppm): porphyrin, δ/ppm, 9.78 (two overlapping doublets, 4H), 8.86 (two overlapped doublets, 4H), 8.06 (s, 4H), 7.88 (s, 2H), 1.56 (s, 36H); phenylethynyl: 8.15 (d, J = 7 Hz, 2H), 7.61 (m, 3H); benzoic acid: 8.25 (d, J = 8 Hz, 2H), 8.16 (d, J = 8 Hz, 2H). Elemental analysis: $C_{65}H_{60}N_4O_2Zn \cdot THF$, calcd C 77.69%, H 6.43%, N 5.25%; found: C 77.69%, H 6.35%, N 5.13%. Mass (MH^+): calcd 992, found 993.

LD2. ^{1}H NMR (THF-d_8 at 1.73 ppm, 3.58 ppm): porphyrin, δ/ppm, 9.89 (d, J = 4 Hz, 2H), 9.79 (d, J = 4 Hz, 2H), 8.96 (d, J = 4 Hz, 2H), 8.94 (d, J = 4 Hz, 2H), 8.14 (s, 4H), 7.93 (s, 2H), 1.60 (s, 36H); naphthalenylethynyl: 9.08 (d, J = 8 Hz, 1H), 8.35 (d, J = 7 Hz, 1H), 8.05 (two overlapping doublets, 2H), 7.82 (t, J = 7 Hz, 1H), 7.71 (t, J = 8 Hz, 1H), 7.67 (t, J = 7 Hz, 1H); benzoic acid: 8.25 (d, J = 8 Hz, 2H), 8.17 (d, J = 8 Hz, 2H). Elemental analysis $C_{69}H_{62}N_4O_2Zn \cdot THF \cdot H_2O$: calcd C 77.27%, H 6.40%, N 4.94%; found: C 77.48%, H 6.59%, N 4.86%. Mass (MH^+) calcd: 1042, found: 1043.

LD3a. ^{1}H NMR (THF-d_8 at 1.73 ppm, 3.58 ppm): porphyrin, δ/ppm, 10.01 (d, J = 4 Hz, 2H), 9.79 (d, J = 4 Hz, 2H), 8.99 (d, J = 4 Hz, 2H), 8.93 (d, J = 4 Hz, 2H), 8.15 (s, 4H), 7.93 (s, 2H), 1.60 (s, 36H); anthracene: 9.32 (d, J = 9 Hz, 2H), 8.69 (s, 1H),

8.21 (d, $J = 9$ Hz, 2H), 7.82 (t, $J = 7$ Hz, 2H), 7.65 (t, $J = 7$ Hz, 2H); benzoic acid: 8.24 (d, $J = 8$ Hz, 2H), 8.17 (d, $J = 8$ Hz, 2H). Elemental analysis $C_{73}H_{64}N_4O_2Zn \cdot 2H_2O$: calcd, C 77.54%, H 6.06%, N 4.95%; found, C 77.36%, H 5.92%, N 4.73%. Mass (MH^+) calcd: 1092, found: 1093.

LD3p. ^{1}H NMR (THF-d_8 at 1.73 ppm, 3.58 ppm): porphyrin, δ/ppm, 9.95 (d, $J = 5$ Hz, 2H), 9.79 (d, $J = 5$ Hz, 2H), 8.98 (d, $J = 5$ Hz, 2H), 8.95 (d, $J = 5$ Hz, 2H), 8.15 (s, overlapping 4H), 7.94 (s, overlapping, 2H); phenanthrenyl-ethynyl: 9.22 (d, $J = 7$ Hz, 2H), 8.95 (d, overlapping, 1H), 8.89 (d, $J = 8$ Hz, 1H), 8.72 (s, 1H), 8.13 (d, overlapping, 1H), 7.95 (t, overlapped, 1H), 7.85(t, $J = 7$ Hz, 1H), 7.78 (two overlapping triplets, 2H); benzoic acid: 8.25 (d, $J = 8$ Hz, 2H), 8.18(d, overlapping, 2H). Elemental analysis $C_{73}H_{64}N_4O_2Zn \cdot H_2O$: calcd, C 78.80%, H 5.98%, N 5.04%; found, C 78.89%, H 6.31%, N 5.03%. Mass (MH^+) calcd: 1092, found: 1093.

LD4. ^{1}H NMR (DMSO-d_6 at 2.50 ppm): porphyrin, δ/ppm, 9.96 (d, $J = 5$ Hz, 2H), 9.79 (d, $J = 5$ Hz, 2H), 8.94 (d, $J = 5$ Hz, 2H), 8.90 (d, $J = 5$ Hz, 2H), 8.08 (s, 4H), 7.91 (s, 2H), 1.58 (s, 36H), pyrene: 9.18 (d, $J = 9$ Hz, 1H), 8.90 (d, overlapping, 1H), 8.60 (d, $J = 9$ Hz, 1H), 8.52 (d, $J = 8$ Hz, 1H), 8.44 (two overlapping doublets, 2H), 8.33 (s, 2H), 8.18 (t, overlapping, 1H); benzoic acid: 8.27 (d, $J = 8$ Hz, 2H), 8.18 (d, $J = 8$ Hz, 2H). Elemental analysis $C_{75}H_{64}N_4O_2Zn$: calcd, C 80.52%, H 5.77%, N 5.01%; found, C 80.34%, H 6.06%, N 4.72. Mass (MH^+) calcd: 1116, found: 1117.

Cell fabrication and characterization of performance

The PSSC devices were fabricated with a working electrode based on TiO_2 nanoparticles (NP) and a Pt-coated counter electrode. For a working electrode, a paste composed of TiO_2 particles (~20 nm)[36] for the transparent nanocrystalline layer was coated on a $TiCl_4$-treated FTO glass substrate (TEC 7, Hartford, USA) to obtain the required thickness on repetitive screen printing. To improve the performance of the PSSC, an additional scattering layer (particle size ≈ 300 nm) was screen-printed on the transparent active layer. Crystallization of TiO_2 films was performed with a programmed procedure: (1) heating at 80 °C for 15 min; (2) heating at 135 °C for 10 min; (3) heating at 325 °C for 30 min; (4) heating at 375 °C for 5 min; (5) heating at 450 °C for 15 min; (6) heating at 500 °C for 15 min. The resulting layer had a transparent layer (thickness ≈ 14 μm) and a scattering layer (thickness ≈ 5 μm), which were treated again with $TiCl_4$ at 70 °C for 30 min and sintered at 500 °C for 30 min. The electrode was then immersed in a porphyrin/THF solution (0.2 mM, 25 °C, 2 h) for dye loading onto the TiO_2 film. The Pt counter electrodes were prepared on spin-coating drops of H_2PtCl_6 solution onto FTO glass and heating at 385 °C for 15 min. To prevent a short circuit, the two electrodes were assembled into a cell of sandwich type and sealed with a hot-melt film (SX1170, Solaronix, thickness 25 μm). The electrolyte solution containing LiI (0.1 M), I_2 (0.05 M), PMII (0.6 M), 4-*tert*-butylpyridine (0.5 M) in a mixture of acetonitrile and valeronitrile (volume ratio 85 : 15) was introduced into the space between the two electrodes, so completing the fabrication of these PSSC devices. The performance of a PSSC device was assessed on measurement of an *I–V* curve with an AM-1.5 G solar simulator (SAN-EI, XES-502S), calibrated with a Si-based reference cell (S1133, Hamamatsu). The incident monochromatic efficiency for conversion from photons to current (IPCE) spectra of the corresponding devices was measured with a system comprising a Xe lamp (PTi A-1010, 150 W), monochromator (PTi, 1200 gr mm^{-1} blazed at 500 nm), and source meter (Keithley 2400, computer-controlled). A standard Si photodiode (ThorLabs FDS1010) served as a reference to calibrate the power density of the light source at each wavelength.

Results and discussion

Molecular design and synthesis

The standard Sonogashira cross-coupling method was used to prepare the cyclic aromatic and the ethynyl substituents, namely phenylethyne, naphthalenylethyne, anthracenylethyne, phenanthrenylethyne, pyrenylethyne and 4-ethynylbenzoic acid.[34,35] For these porphyrins, zinc porphine acts as the primary chromophore. 3,5-Di-*tert*-butyl-phenyl groups increase the solubility, suppress dye aggregation, and protect the porphine core structure. The advantage of this design is that all LD porphyrins are prepared in two steps from a brominated porphyrin.

UV-visible absorption and fluorescence spectra

Fig. 1 shows UV-visible spectra of PE1 and LD porphyrins in THF. Fig. 2 compares UV-visible spectra of LD porphyrins in THF and those on TiO_2 films. Fig. 3 shows fluorescence spectra of LD porphyrins in THF. The wavelengths of maxima in the UV-visible absorption and fluorescence spectra are reported in Table 1.

Fig. 1 shows that PE1 and LD porphyrins all exhibit typical porphyrin absorption characteristics:[37] strong B bands were found near 450 nm, whereas weak Q bands were observed near 670 nm. For LD porphyrins in solution, the maxima of B bands were red-shifted from 439 nm of PE1 to LD1's 450, LD2's 453, LD3a's 468, LD3p's 454 and LD4's 464 nm (Table 1). As for the Q absorptions: the splitted Q bands of PE1 at 567 and 616 nm

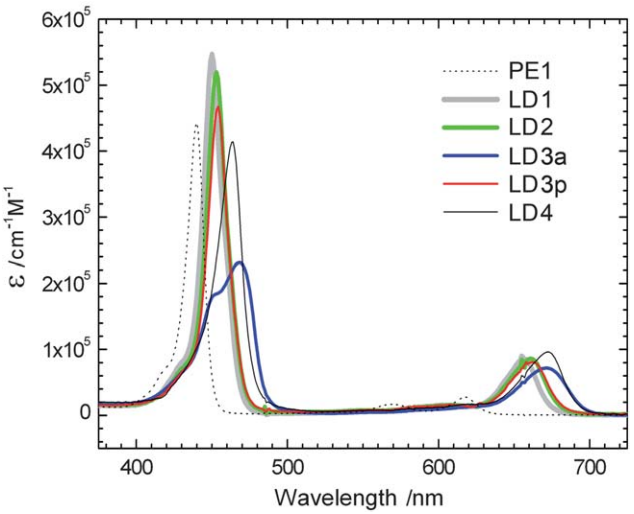

Fig. 1 Absorption spectra of PE1 and LD porphyrins in THF.

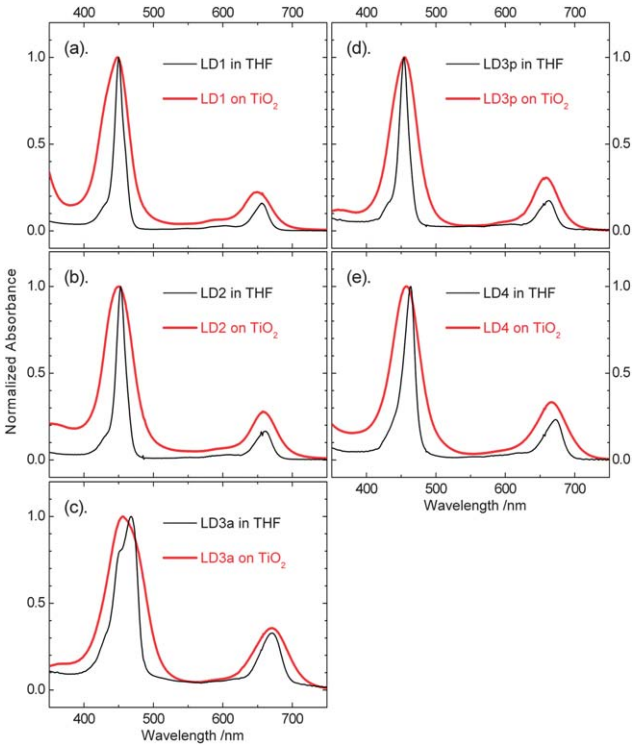

Fig. 2 Normalized UV-visible spectra of LD porphyrins in THF (black curves) and on TiO_2 films in air (red curves).

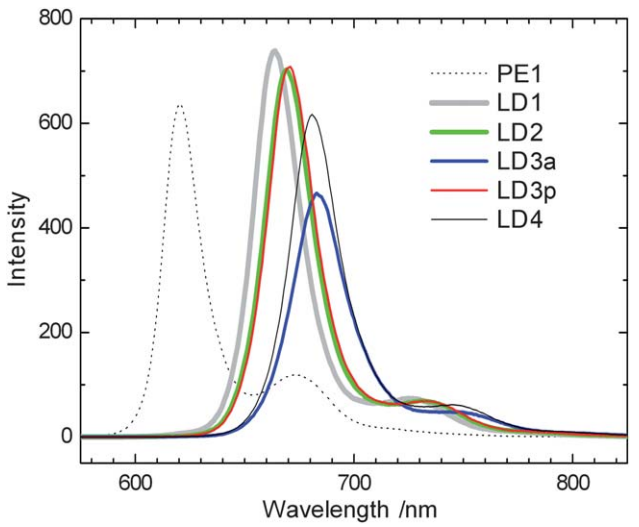

Fig. 3 B band-excited fluorescent emission spectra of PE1 and LD porphyrins (2×10^{-6} M in THF).

were merged and red-shifted to 656, 661, 671, 662 and 672 nm for LD1, LD2, LD3a, LD3p, and LD4, respectively. These spectral changes are consistent with the literature reports,[27,38,39] and they can be interpreted to be LD zinc porphyrins having decreased symmetry and extended π-conjugation according to the Gouterman's model.[37,40] Among the LD porphyrins, the absorptions of LD3a and LD4 are more red-shifted and broadened than those of other porphyrins in the series, reflecting that electronic coupling between the chromophore and the porphine core was more significant for LD3a and LD4 than for the others.

Table 1 Absorption wavelength, fluorescence maxima and first porphyrin-ring reduction potentials of PE1 and LD porphyrins in THF

Dye	Absorption/nm (log $\varepsilon/10^5$ M^{-1} cm^{-1})	Emission/nm[a]	$E_{1/2}$/V *vs.* SCE[c]
PE1[b]	439 (5.64), 567 (4.21), 616 (4.41)	621, 674	−1.23
LD1	450 (5.69), 656 (4.93)	663, 728	−1.09
LD2	453 (5.72), 661 (4.93)	669, 733	−1.07
LD3a	468 (5.36), 671 (4.86)	685, 751	−1.04
LD3p	454 (5.67), 662 (4.91)	671, 733	−1.04
LD4	464 (5.62), 672 (4.98)	681, 748	−1.02

[a] Excitation wavelength/nm: PE1 439, LD1 450, LD2 453, LD3a 468, LD3p 454, and LD4 464. [b] Taken from ref. 21. [c] 0.5 mM of LD porphyrins in THF/0.1 M TBAP/N_2; Pt working and counter electrodes; SCE reference electrode; scan rate = 100 mV s^{-1}.

Fig. 2 compares absorption spectra of the LD porphyrins in THF with those on TiO_2 films. To avoid saturation of the B-band absorption in these spectra, only small amounts of the porphyrins were allowed to adsorb onto the TiO_2 films (*i.e.* porphyrin dyes were partially loaded). In addition, the absorption spectra were normalized to make a comparison between the two conditions. The results indicate that the B and Q bands of LD/TiO_2 films were only slightly shifted but considerably broadened relative to the solution spectra. The broadened absorption bands of the thin-film samples might reflect intermolecular interactions of molecules aggregated on the TiO_2 surfaces. The feature of the blue shoulders of B bands previously observed for PE-series porphyrins[21,22,41] was not discernible in the spectra of the LD/TiO_2 film. As these blue shoulders represent H-type aggregation of porphyrins on surfaces of TiO_2 nanoparticles, the lack of such feature suggests that H-type aggregation of LD porphyrins on TiO_2 might be insignificant.

For the fluorescence spectra in solution (Fig. 3), major emissions of LD porphyrins were observed at LD1 663, LD2 669, LD3a 685, LD3p 671 and LD4 681 nm. The fluorescence intensities are comparable among all these LD porphyrins. The trend for the LD emissions in being red-shifted relative to PE1 is similar to the trend of the Q band absorption spectra. The spectrum of LD3p is similar to that of LD2 rather than to that of its isomer LD3a, which shows a further red-shifted feature. This phenomenon indicates that electronic coupling between anthracene and the porphyrin ring was more effective than that between phenanthrene and the porphyrin ring.

Electrochemical properties and DFT calculations

Fig. 4 displays cyclic voltammograms (CV) of LD porphyrins in THF/TBAP; the resulting reduction potentials are collected in Table 1.

The first porphyrin-ring reductions of LD porphyrins are found at LD1 −1.09, LD2 −1.07, LD3a −1.04, LD3p −1.04 and LD4 −1.02 V *vs.* SCE as *quasi*-reversible reactions. These potentials are positively shifted from that of PE1 porphyrin (−1.23V *vs.* SCE),[21] indicating the effect of extended π-conjugation. The ease of reduction of the series occurs in the order pyrene (LD4) > anthracene (LD3a) ≈ phenanthrene (LD3p) > naphthalene (LD2) > benzene (LD1). This trend is consistent with the conjugation length of each substituent. Oxidation reactions of LD porphyrins in THF/TBAP were observed to be

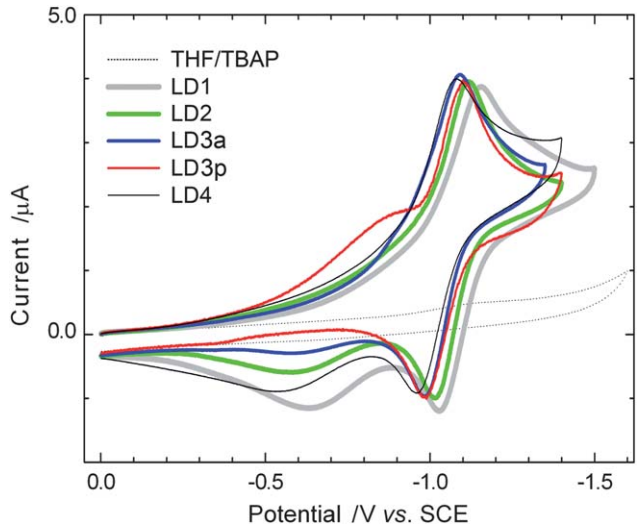

Fig. 4 Cyclic voltammograms of LD porphyrins (0.5 mM) in THF/0.1 M TBAP.

nearly irreversible. For this reason, the potential levels of HOMO for each LD porphyrin were obtained from E(HOMO) = E(LUMO) + $E_{0\text{–}0}$; E(LUMO) = E_{red} was determined from the CV measurements and $E_{0\text{–}0}$ is the zero–zero excitation energy obtained from the intersection of the corresponding normalized absorption and emission spectra.[21,27,28,42] Fig. 5 shows an energy-level diagram of LD porphyrins to compare the HOMO/LUMO levels of each porphyrin with respect to the valence band (VB) and conduction band (CB) of TiO_2. This diagram shows that the LUMO levels of LD porphyrins become increasingly stabilized with an increasing number of aromatic rings. Although the LUMO level of LD4 is the least in the series, it is still above the CB level of TiO_2. Our results indicate that LUMO levels of all

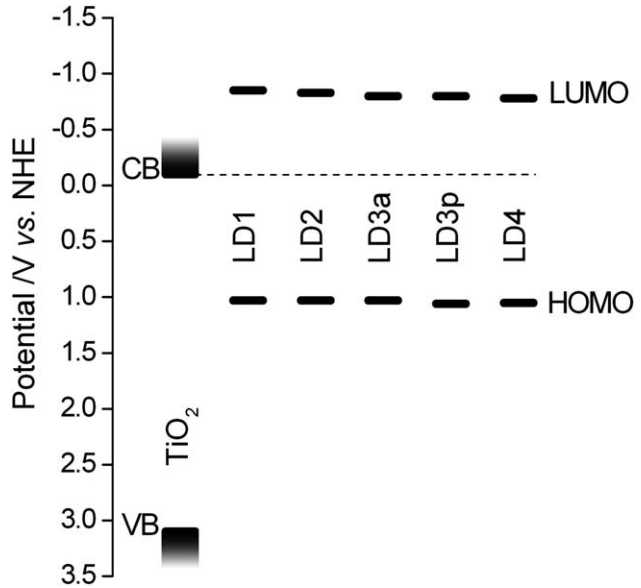

Fig. 5 An energy-level diagram of LD porphyrins and TiO_2; E(LUMO) = E_{red} and E(HOMO) = E(LUMO) + $E_{0\text{–}0}$.

LD porphyrins should be capable of injecting electrons into the CB of TiO_2.

To assist our qualitative understanding of the electrochemical behavior of LD porphyrins, we performed DFT calculations at the B3LYP/LanL2DZ level of theory.[43] As shown in Fig. 6, the MO patterns of LD porphyrins are consistent with those of Gouterman's four-orbital model,[37] *i.e.* HOMO-1 and HOMO resemble those of the a_{1u} and a_{2u} orbitals whereas the LUMO and LUMO + 1 are similar to those of the e_g orbitals. These patterns are consistent also with the suggestion that the first reduction and oxidation of LD are reactions centered on the porphyrin ring. The HOMO and LUMO patterns exhibit, however, a feature with slight delocalization to the anchoring group and the cyclic aromatic substituents. This deviation from Gouterman's four-orbital model is rationalized through a decreased symmetry of the complexes and an extended π-conjugation of the substituent. This condition is consistent with the potential shifts of LD relative to PE1 porphyrin. Our results indicate that the electronic densities of HOMO and HOMO-1 of LD3a extend to the entire anthracene moiety whereas those of LD3p extend only partially to the phenanthrene moiety. This condition is consistent with the spectral observations for which LD3a exhibits a more red-shifted feature than LD3p through superior π-conjugation of LD3a.

The delocalization of the HOMO and LUMO patterns of the LD porphyrins also suggests that the auxochromic substituents (benzene through pyrene) of the LD porphyrins should be considered as part of the molecules instead of being treated as donor groups. As such, stepwise intramolecular charge transfer should not be expected for the LD dyes upon excitation. The concept of stepwise intramolecular charge transfer was originally reported by Haque *et al.* for ruthenium dyes with distance-controlled electron-donor groups.[44] Comparison of the LD porphyrins with Haque's Ru dyes suggests that such an effect should not play a role for the LD devices because of the much less electron-donating substituents and the delocalized HOMO/LUMO patterns. The HOMO patterns of Haque's Ru dyes were reported to be localized at the electron-donating phenylamine moieties.

Photovoltaic properties

Porphyrins LD1–LD4 were sensitized onto TiO_2 films to serve as working electrodes for photovoltaic characterizations; the corresponding current–voltage characteristics and the IPCE action spectra are shown in Fig. 7a and b, respectively; the resulting photovoltaic parameters are summarized in Table 2. In relation to our previous work,[21,27,28] the performances of the LD1–LD4 devices are greatly improved with the following advances. First, the small-resistance FTO substrates were used for both working and counter electrodes. Second, the thickness of the TiO_2 active layer increased from 12 μm to 14 μm. Third, a scattering layer of thickness 5 μm was added on top of the active layer. Finally, the $TiCl_4$ post-treatment was performed for all TiO_2 films before dye sensitization. As a result, the efficiency of power conversion of the N719-based device serving as a reference was enhanced from the previous 7.0%[28] to the present 9.3%. As summarized in Table 2, the device performances of porphyrins in this series show an order LD4 > LD3p > LD2 > LD3a > LD1, for which the best

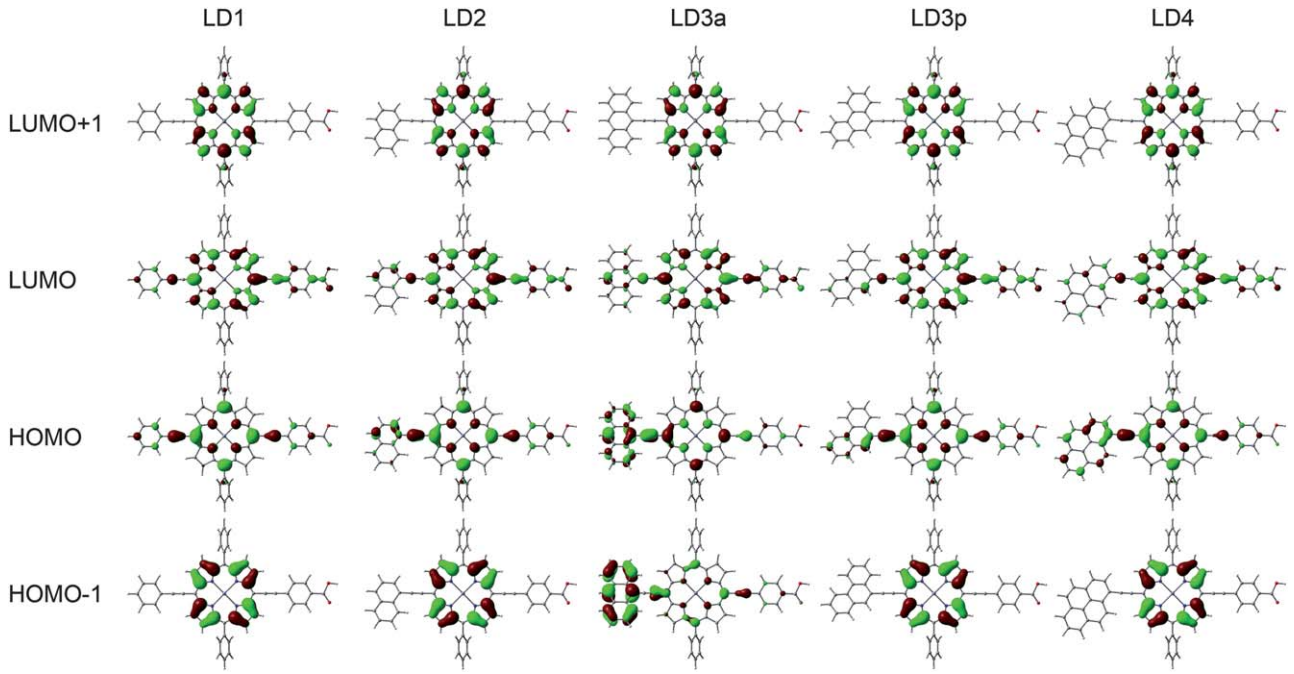

Fig. 6 Molecular-orbital patterns of LD porphyrins with the geometry of each molecule optimized at the B3LYP/LanL2DZ level of theory.

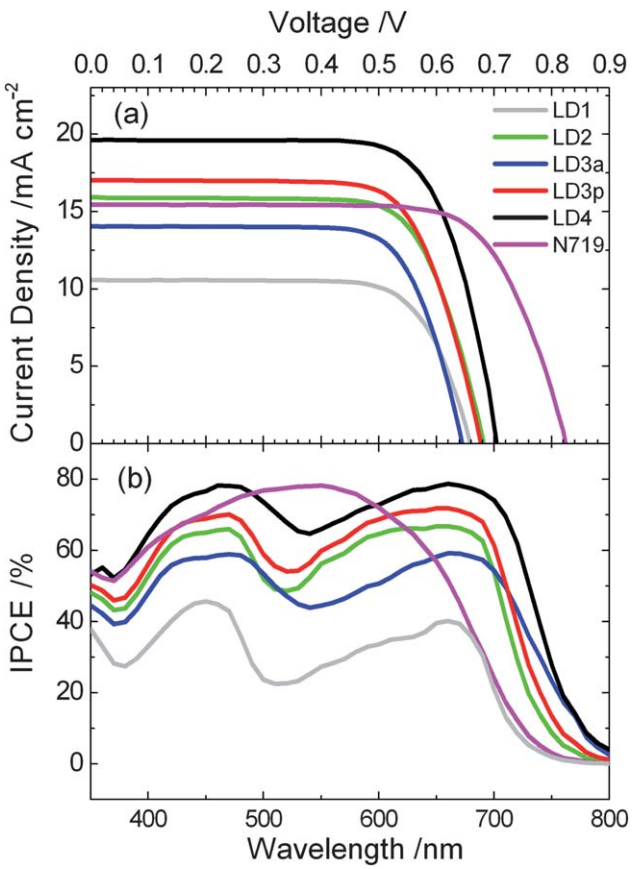

Fig. 7 (a) Current–voltage characteristics of LD-sensitized solar cells and N719 cell; (b) corresponding IPCE action spectra.

Table 2 Photovoltaic parameters of LD-sensitized solar cells[a]

Dye	J_{SC} mA cm^{-2}	V_{OC}/V	FF	η (%)
LD1[b]	10.562	0.660	73.30	5.11
LD2	15.921	0.682	72.08	7.83
LD3a	14.044	0.654	73.11	6.62
LD3p	17.019	0.678	71.62	8.26
LD4	19.627	0.711	72.09	10.06
N719[c]	15.440	0.828	72.50	9.27

[a] Under AM1.5 illumination (power 100 mW cm^{-2}) with an active area of 0.16 cm^2. [b] Typical dye-loading amounts per nmol per cm^2 of LD-sensitized solar cells are LD1 90, LD2 96, LD3a 107, LD3p 113, and LD4 109. [c] As a reference, the overall efficiency of N719 sensitized solar cell was determined.

dye LD4 features J_{SC}/mA cm^{-2} = 19.627, V_{OC}/V = 0.711 and FF = 0.721, with overall efficiency η = 10.06% of power conversion, which outperforms that of a N719-based DSSC fabricated using the same working and counter electrodes.[45]

As mentioned before, the anthracene substituent has effective π-conjugation to red-shift and to broaden the UV-visible absorption bands for porphyrin LD3a, but the performance of the LD3a device was worse than that of LD3p and even the LD2 cell. The inferior performance of the LD3a device is understood to be due to its smaller IPCE values (which decrease J_{SC}). This result might be attributed to the following two reasons. First, the absorption coefficients of LD3a are smaller than the other LD porphyrins (Fig. 2). Under similar dye-loading conditions, the light-harvesting efficiencies of LD3a are expected to be less than those of the other LD porphyrins, leading to smaller IPCE for the LD3a device. Second, the 9 and 10 carbons of anthracene are reported to be more susceptible to oxidation than phenanthrene or pyrene, generating anthraquinone.[46] As a result, the

anthracenyl substituent of LD3a might be more chemically reactive upon charge separation, which hampers the dye regeneration.

The superior photovoltaic performance of the LD4-based PSSC can be attributed to its enhanced light harvesting ability. As shown in Fig. 7b, the IPCE action spectrum of the LD4-based PSSC covers the entire visible spectral region and further extends beyond 800 nm, which outperforms that of N719. In addition, the IPCE values of LD4-PSSC are clearly higher than those of the other LD porphyrins, contributing to its improved overall efficiency. However, V_{OC} of device LD4 was much smaller than that of cell N719, and this property is reported to be due to much smaller electron lifetimes for porphyrin-based solar cells than for the N719 cells.[47] The smaller V_{OC} of PSSC thus reflects a decreased electron lifetime related to a rapid recombination of electrons with I_3^- ions in the electrolyte (electron interception). The value of V_{OC} for a push–pull porphyrin dye such as YD2[16] is greater than those of LD porphyrins; this effect might be rationalized by the electron interception that is more efficient for LD porphyrins than for push–pull porphyrins because of improved charge separation for the latter. This condition leaves room for improvement of the cell performance for a PSSC to enhance its V_{OC} *via* molecular design based on the structure of LD4 incorporating electron-donor groups in appropriate positions.

Conclusions

To examine the effects of cyclic aromatic substituents on the photovoltaic performance of the corresponding PSSC, we prepared zinc porphyrins bearing a phenylethynyl, naphthalenylethynyl, anthracenylethynyl, phenanthrenyl-ethynyl or pyrenylethynyl substituents, denoted LD1, LD2, LD3a, LD3p or LD4, respectively. LD3a and LD4 yield the most red-shifted and broadened UV-visible absorption and fluorescence bands in the series. Electrochemical tests show that LD4 is the most readily reduced species. The combination of both spectral and electrochemical results predicts the potentials of the HOMO and the LUMO levels with an order LD1 > LD2 > LD3a > LD3p > LD4. The electron distributions of frontier orbitals predicted with DFT calculations indicate that there exists a driving force for LD porphyrins to push the electrons from the cyclic aromatic substituents toward the anchoring group that is attached to TiO_2. As for the photovoltaic performance of LD-sensitized solar cells, there exhibits a systematic trend with LD4 (10.06%) > LD3p (8.26%) > LD2 (7.83%) > LD3a (6.62%) > LD1 (5.11%), so that the performance of the LD4 cell is superior to that of a N719 cell. The superior cell performance of LD4 is rationalized to be due to the broader and more red-shifted spectral feature that makes the IPCE spectrum to cover broadly across the entire 400–800 nm region and yields a J_{SC} value over 19 mA cm^{-2} under one-sun illumination. As a result, the enhanced light harvesting ability across the entire visible region renders LD4 the most efficient photo-sensitizer in the series. The smaller V_{OC} might be further improved on attaching a donor group in an appropriate position of the porphyrin. We emphasize the significance of the present work with an enhanced light-harvesting ability for PSSC involving cyclic aromatic hydrocarbon substituents on the opposite side of the anchoring group of a porphyrin dye.

Acknowledgements

National Science Council of Taiwan and Ministry of Education of Taiwan, under the ATU program, provided support for this project.

Notes and references

1 M. K. Nazeeruddin, P. Péchy and M. Grätzel, *Chem. Commun.*, 1997, 1705–1706.
2 M. K. Nazeeruddin, S. M. Zakeeruddin, R. Humphry-Baker, M. Jirousek, P. Liska, N. Vlachopoulos, V. Shklover, C.-H. Fischer and M. Grätzel, *Inorg. Chem.*, 1999, **38**, 6298–6305.
3 M. K. Nazeeruddin, P. Péchy, T. Renouard, S. M. Zakeeruddin, R. Humphry-Baker, P. Comte, P. Liska, L. Cevey, E. Costa, V. Shklover, L. Spiccia, G. B. Deacon, C. A. Bignozzi and M. Grätzel, *J. Am. Chem. Soc.*, 2001, **123**, 1613–1624.
4 T. W. Hamann, R. A. Jensen, A. B. F. Martinson, H. V. Ryswykac and J. T. Hupp, *Energy Environ. Sci.*, 2008, **1**, 66–78.
5 L. M. Goncalves, V. de Zea Bermudez, H. A. Ribeiro and A. M. Mendes, *Energy Environ. Sci.*, 2008, **1**, 655–667.
6 M. K. Nazeeruddin, F. De Angelis, S. Fantacci, A. Selloni, G. Viscardi, P. Liska, S. Ito, B. Takeru and M. Grätzel, *J. Am. Chem. Soc.*, 2005, **127**, 16835–16847.
7 M. Grätzel, *Inorg. Chem.*, 2005, **44**, 6841–6851.
8 F. Gao, Y. Wang, D. Shi, J. Zhang, M. Wang, X. Jing, R. Humphry-Baker, P. Wang, S. M. Zakeeruddin and M. Grätzel, *J. Am. Chem. Soc.*, 2008, **130**, 10720–10728.
9 W. M. Campbell, A. K. Burrell, D. L. Officer and K. W. Jolley, *Coord. Chem. Rev.*, 2004, **248**, 1363–1379.
10 H. Imahori, T. Umeyama and S. Ito, *Acc. Chem. Res.*, 2009, **42**, 1809–1818.
11 H. Imahori, Y. Matsubara, H. Iijima, T. Umeyama, Y. Matano, S. Ito, M. Niemi, N. V. Tkachenko and H. Lemmetyinen, *J. Phys. Chem. C*, 2010, **114**, 10656–10665.
12 N. R. de Tacconi, W. Chanmanee, K. Rajeshwar, J. Rochford and E. Galoppini, *J. Phys. Chem. C*, 2009, **113**, 2996–3006.
13 W. M. Campbell, K. W. Jolley, P. Wagner, K. Wagner, P. J. Walsh, K. C. Gordon, L. Schmidt-Mende, M. K. Nazeeruddin, Q. Wang, M. Grätzel and D. L. Officer, *J. Phys. Chem. C*, 2007, **111**, 11760–11762.
14 A. Allegrucci, N. A. Lewcenko, A. J. Mozer, L. Dennany, P. Wagner, D. L. Officer, K. Sunahara, S. Moric and L. Spiccia, *Energy Environ. Sci.*, 2009, **2**, 1069–1073.
15 T. Bessho, S. M. Zakeeruddin, C.-Y. Yeh, E. W.-G. Diau and M. Gratzel, *Angew. Chem., Int. Ed.*, 2010, **49**, 6646–6649.
16 S.-L. Wu, H.-P. Lu, H.-T. Yu, S.-H. Chuang, C.-L. Chiu, C.-W. Lee, E. W.-G. Diau and C.-Y. Yeh, *Energy Environ. Sci.*, 2010, **3**, 949–955.
17 G. Calogero, G. DiMarco, S. Caramori, S. Cazzanti, R. Argazzi and C. A. Bignozzi, *Energy Environ. Sci.*, 2009, **2**, 1162–1172.
18 J. K. Park, J. Chen, H. R. Lee, S. W. Park, H. Shinokubo, A. Osuka and D. Kim, *J. Phys. Chem. C*, 2009, **113**, 21956–21963.
19 C. Y. Lee, C. She, N. C. Jeong and J. T. Hupp, *Chem. Commun.*, 2010, **46**, 6090–6092.
20 I. Radivojevic, A. Varotto, C. Farleya and C. M. Drain, *Energy Environ. Sci.*, 2010, **3**, 1897–1909.
21 C.-Y. Lin, C.-F. Lo, L. Luo, H.-P. Lu, C.-S. Hung and E. W.-G. Diau, *J. Phys. Chem. C*, 2009, **113**, 755–764.
22 C.-F. Lo, L. Luo, E. W.-G. Diau, I.-J. Chang and C.-Y. Lin, *Chem. Commun.*, 2006, 1430–1432.
23 L. Luo, C.-J. Lin, C.-Y. Tsai, H.-P. Wu, L.-L. Lin, C.-F. Lo, C.-Y. Lin and E. W.-G. Diau, *Phys. Chem. Chem. Phys.*, 2010, **12**, 1064–1071.
24 L. Luo, C.-J. Lin, C.-S. Hung, C.-F. Lo, C.-Y. Lin and E. W.-G. Diau, *Phys. Chem. Chem. Phys.*, 2010, **12**, 12973–12977.
25 C.-W. Chang, L. Luo, C.-K. Chou, C.-F. Lo, C.-Y. Lin, C.-S. Hung, Y.-P. Lee and E. W.-G. Diau, *J. Phys. Chem. C*, 2009, **113**, 11524–11531.
26 L. Luo, C.-F. Lo, C.-Y. Lin, I.-J. Chang and E. W.-G. Diau, *J. Phys. Chem. B*, 2006, **110**, 410–419.
27 C.-Y. Lin, Y.-C. Wang, S.-J. Hsu, C.-F. Lo and E. W.-G. Diau, *J. Phys. Chem. C*, 2010, **114**, 687–693.

28 C.-F. Lo, S.-J. Hsu, C.-L. Wang, Y.-H. Cheng, H.-P. Lu, E. W.-G. Diau and C.-Y. Lin, *J. Phys. Chem. C*, 2010, **114**, 12018–12023.
29 T.-I. Ho, A. Elangovan, H.-Y. Hsu and S.-W. Yang, *J. Phys. Chem. B*, 2005, **109**, 8626–8633.
30 B. N. Boden, K. J. Jardine, A. C. W. Leung and M. J. MacLachlan, *Org. Lett.*, 2006, **8**, 1855–1858.
31 C.-W. Wan, A. Burghart, J. Chen, F. Bergstrom, L. B.-A. Johansson, M. F. Wolford, T. G. Kim, M. R. Topp, R. M. Hochstrasser and K. Burgess, *Chem.–Eur. J.*, 2003, **9**, 4430–4441.
32 O. Taratula, J. Rochford, P. Piotrowiak, E. Galoppini, R. A. Carlisle and G. J. Meyer, *J. Phys. Chem. B*, 2006, **110**, 15734–15741.
33 P. G. Hoertz, R. A. Carlisle and G. J. Meyer, *Nano Lett.*, 2003, **3**, 325–330.
34 K. Sonogashira, Y. Tohda and N. Hagihara, *Tetrahedron Lett.*, 1975, 4467–4470.
35 S. Takahashi, Y. Kuroyama and K. Sonogashira, *Synthesis*, 1980, 627–630.
36 S. Ito, P. Chen, P. Comte, M. K. Nazeeruddin, P. Liska, P. Péchy and M. Grätzel, *Progr. Photovolt.: Res. Appl.*, 2007, **15**, 603.
37 M. Gouterman, *J. Mol. Spectrosc.*, 1961, **6**, 138.
38 M.-C. Kuo, L.-A. Li, W.-N. Yen, S.-S. Lo, C.-W. Lee and C.-Y. Yeh, *Dalton Trans.*, 2007, 1433–1439.
39 P. N. Taylor, A. P. Wylie, J. Huuskonen and H. L. Anderson, *Angew. Chem., Int. Ed.*, 1998, **37**, 986–989.
40 Based on Gouterman's conclusion, we would expect the Q bands of the free-base LD porphyins to become splitted again due to the further lowered symmetry of the free-base porphyrins than that of the LD zinc porphyrins.[37] Such a behaviour has been observed for other metallo- *vs.* free-base ethynyl-substituted porphyrins, *e.g.*,C.-Y. Lin, Y.-C. Chen, C.-W. Yao, S.-C. Huang and Y.-H. Cheng, *Dalton Trans.*, 2008, 793–799.
41 M. Kasha, *Radiat. Res.*, 1963, **20**, 55–71.
42 M. Grätzel, *Nature*, 2001, **414**, 338–344.
43 M. J. Frisch, et al., *Gaussian 03, Revision D.01*, Gaussian, Inc., Pittsburgh PA, 2003. All IR frequencies were checked to be positive.
44 S. A. Haque, S. Handa, K. Peter, E. Palomares, M. Thelakkat and J. R. Durrant, *Angew. Chem., Int. Ed.*, 2005, **44**, 5740–5744.
45 The dye-loading condition and the electrolyte for N719 differ from those for the porphyrins: the electrode was immersed into a dye solution containing N719 (300 μM) and CDCA(300 μM) in the mixture of acetonitrile and *tert*-butanol (volume ratio: 1/1) overnight. The electrolyte is Z960.
46 M. L. Merlau, S.-H. Cho, S.-S. Sun, S. T. Nguyen and J. T. Hupp, *Inorg. Chem.*, 2005, **44**, 5523–5529.
47 A. J. Mozer, P. Wagner, D. L. Officer, G. G. Wallace, W. M. Campbell, M. Miyashita, K. Sunahara and S. Mori, *Chem. Commun.*, 2008, 4741.